European Review for Medical and Pharmacological Sciences 2022; 26: 422-431

MiR-486 alleviates hypoxia/reoxygenation-induced H9c2 cell injury by regulating forkhead box D3

N. WANG[1], Y.-B. YU[2]

[1]Department of Geriatrics, Beijing Friendship Hospital, Capital Medical University, Beijing, China
[2]Intensive Care Unit, Beijing Friendship Hospital, Capital Medical University, Beijing, China

Abstract. – OBJECTIVE: Myocardial ischemia-reperfusion injury (IRI) is common in myocardial infarction and is the leading cause of death. Therefore, we investigated the effect of miR-486 on myocardial IRI to explore new targets for clinical treatment of IRI.

MATERIALS AND METHODS: We made a rat myocardial IRI model by obstructing the coronary arteries and detected the change of miR-486 expression in rat myocardial tissue. In addition, we induced injury of rat cardiomyocytes (H9c2 cells) by hypoxia/reoxygenation and transfected H9c2 cells with agomir-miR-486 and antagomir-miR-486 to detect the effects of miR-486 on the viability, inflammation and apoptosis of cardiomyocytes. We also used the Targetscan system to predict the direct target of miR-486 and verified the effect of miR-486 on downstream targets through the Dual-Luciferase reporter assay.

RESULTS: HE staining and the detection of myocardial injury markers and inflammatory factors verified the effectiveness of IRI rat model. The expression of miR-486 in myocardium of IRI rats was significantly lower than that of the control group. The overexpression of miR-486 in H9c2 cells increased the viability of H9c2 cells and reduced the levels of inflammation and apoptosis. MiR-486 is predicted to have a potential binding site to forkhead box D3 (FOXD3). The Dual-Luciferase reporter assay proved that miR-486 can bind and degrade FOXD3 mRNA. In addition, the overexpression of FOXD3 was found to attenuate the protective effect of miR-486 on H9c2 cells.

CONCLUSIONS: MiR-486 protects cardiomyocytes and reduces the levels of inflammation and apoptosis by binding and inhibiting FOXD3 activity. Therefore, miR-486 may become a new target for myocardial IRI therapy.

Key Words:
Myocardial ischemia-reperfusion injury, MiR-486, Forkhead box D3.

Introduction

Acute myocardial infarction is an acute manifestation of coronary heart disease and the leading cause of death[1]. Its basic pathological changes are rupture of coronary plaques, reduction of thrombosis, and even interruption of blood supply, which eventually leads to severe ischemic and hypoxic lesions in some myocardial tissues[2]. If the blood flow of the occluded blood vessel is not restored, the myocardial tissue in the infarct-related area will be necrotic[3]. Timely reperfusion strategies, such as drug thrombolysis, percutaneous coronary intervention, and coronary artery bypass grafting, can help open occluded blood vessels as early as possible and effectively rescue ischemic myocardial tissue[4]. Therefore, traditional reperfusion strategies have reduced the infarct size and improved cardiac function to a certain extent, which has greatly improved the prognosis of patients. However, with further research on the process of myocardial ischemia and reperfusion, the researchers found that although reperfusion therapy can regain blood perfusion in ischemic myocardium in a short time, reperfusion therapy itself can also lead to more severe dysfunction and structural damage after myocardial ischemia[5]. This phenomenon is called myocardial ischemia-reperfusion injury (IRI). Herr et al[6] has found that IRI-induced myocardial infarction area can account for 50% of the final infarct size. IRI can cause the destruction of myocardial cell membrane, and then cause an enlargement of the range of myocardial infarction. Then, IRI causes myocardial contraction and diastolic function to decrease, manifested as malignant arrhythmias, cardiac insufficiency and even sudden death[6]. In

Corresponding Author: Yanbo Yu, MM; e-mail: yyyyjycyu@126.com

addition, IRI can cause microcirculation disorders in up to 50% of patients undergoing percutaneous coronary intervention, which seriously affects the treatment effect and the patient's prognosis[7]. Therefore, how to reduce IRI has become the focus and hot issue in the field of coronary heart disease research.

Micro RNA (miRNA) is a class of endogenous and regulatory small molecule non-coding RNA, containing about 20-25 nucleotides[8]. Among them, the miR-486 family, as a regulator of gene transcription, can regulate the expression of specific target genes and participate in the pathological processes of various diseases[9]. Chai et al[10] has shown that miR-486-5p can inhibit the inflammatory response of human nucleus pulposus cells and the degradation of extracellular matrix by regulating forkhead box protein O1, thereby reducing the apoptosis of nucleus pulposus cells[10]. In addition, miR-486 has also been found to regulate the proliferation and apoptosis of a variety of tumor cells[11,12]. Although miR-486 plays an indispensable role in the pathological process of various diseases, the role of miR-486 in myocardial IRI has not yet been elucidated. In our current study, we found that the expression of miR-486 was lower in myocardial tissue of IRI rats. Given above, we aimed to investigate the effect and mechanism of miR-486 on rat myocardial tissues and cells through transfection technology.

Materials and Methods

Animals

We selected 30 male specific pathogen free Sprague Dawley rats (8-10 weeks of age, 180-200 g) for this study. Rats were purchased and bred at Capital Medical University Animal Center. Room temperature of about 22°C, relative humidity of 55% and 12 hours of alternating light were maintained in the animal house. Clean breeding and drinking water are available regularly. This study was approved by the Animal Ethics Committee of Capital Medical University Animal Center.

Myocardial IRI Model

After anesthetizing rats with 2% sodium pentobarbital (40 mg/kg), we placed them on the operating table. Then, we used scissors to cut off the fur on the chest area and disinfect the chest skin with iodine. After cutting the skin and trachea of the rat's neck using sterile scissors, we connected animal ventilator (CWE SAR-830, Orange, CA, USA) to rats and set the heart rate of 80-100/min, the breathing rate of 60/min, the breathing ratio of 1:1.5 and the tidal volume of 70 mL. We cut the skin and ribs of the left chest of the rat using scissors, and then cut the capsule and exposed the heart. We used sterile sutures to ligate the left anterior descending coronary artery between the pulmonary artery cone and the left atrial appendage. Cyanosis of the epicardium at the distal end of the ligation and ST segment elevation of the electrocardiogram (ECG) indicated myocardial ischemia. After 30 min of ischemia, we loosened the ligature to open the coronary arteries for another 180 min. The fall of the ST segment of the ECG indicated successful reconnection. Rats in the Sham group only exposed the heart without ligating the coronary arteries. Finally, we euthanized the rats and collected blood and heart tissue.

Histology and Hematoxylin-eosin (HE) Staining

After the rat heart tissue was cleaned with normal saline, we immersed the heart tissue in 4% paraformaldehyde for 24-48 h. We put heart tissue into gradient alcohol, xylene, and paraffin, and made paraffin blocks. We then cut the paraffin mass into 5 μm paraffin sections using a microtome (LEICA RM2235, Koln, Germany). Paraffin sections were baked in a 37°C incubator for 24-72 h and stored at room temperature.

Before HE staining, we first baked paraffin sections in a 55 °C incubator for 1 h. We then placed the sections in xylene and gradient alcohol. After rinsing the sections with running water, we put the sections in hematoxylin staining solution (Beyotime, Shanghai, China) for 1 min, and then differentiate the tissue with hydrochloric acid alcohol for 3 s. After rinsing the sections with running water, we put the sections in eosin staining solution (Beyotime, Shanghai, China) for 1 min and continued dehydration with gradient alcohol. Finally, we used neutral balsam for mounting and observed the staining results using an optical microscope.

2, 3, 5-Triphenyl Tetrazolium Chloride (TTC) Staining

We collected rat heart tissue and washed the heart with normal saline. Then, we put the heart tissue in a refrigerator at -20°C for about 20 min. Then, we cut the heart tissue into 5-6 pieces starting from the apex of the heart. The thickness of each piece was about 2 mm. We then placed the sections in 1% TTC stain (Beyotime, Shanghai, China) and incubated tissue at 37°C for 15-30

min. We then used the camera to take pictures and analyze the extent of myocardial ischemia. Normal tissue was red and ischemic tissue was pale. The area of myocardial ischemia was represented as a percentage of the area of the left ventricle.

Detection of Lactic Dehydrogenase (LDH) and Creatine Kinase (CK)

After 180 min of reperfusion in rats, we took about 2 mL of abdominal aortic blood from the rats and collected the serum by centrifugation. Then, we used LDH detection kit (Beyotime, Shanghai, China) and CK detection kit (Beyotime, Shanghai, China) to detect LDH and CK activity in rat serum. We first added matrix buffer and 5 μL of Coenzyme to the blood sample. After 15 min, we added 25 μL of dinitrophenylhydrazine to the mixture and incubated them for 15 min at 37°C. We then added 250 μL of NaOH to the mixture and incubated them for 5 min. Finally, we use a spectrophotometer to measure the absorbance at 450 nm and calculate the LDH activity. The detection of CK activity is similar to that of LDH.

Cell Culture and Hypoxia/Reoxygenation (H/R) Model

Rat myocardial cell line (H9c2 cells) (American Type Culture Collection, ATCC, Manassas, VA, USA) was used in this study. We used Dulbecco's Modified Eagle's Medium (DMEM; Gibco, Rockville, MD, USA) containing 10% fetal bovine serum (FBS: Gibco, Rockville, MD, USA) and 1% double antibody (penicillin plus streptomycin) (Gibco, Rockville, MD, USA) to culture H9c2 cells and cultured H9c2 cells in a 37°C incubator containing 5% CO_2. All cell experiments were performed in a sterile cell clean bench. Agomir-control, agomir-miR-486, antagomir-control, antagomir-miR-486, lenti-control and lenti-FOXD3 are designed in Shanghai Genepharma Company (Shanghai, China). We used Lipofectamine 2000 (Invitrogen, Carlsbad, CA, USA) for cell transfection following the manufacturer's instructions.

We put the sugar-free D-Hank's liquid container in an anaerobic incubator (95% N_2 and 5% CO_2) for 30 min to make the oxygen concentration in the liquid less than 1%. Then, we selected the cells in the logarithmic growth phase and washed them 3 times with sugar-free D-Hank's solution. We then cultured the cells using sugar-free DMEM medium and placed the cells in the anaerobic incubator. After 4 h, we re-cultured the cells with normal medium.

Cell Counting Kit 8 (CCK8) Assay

We cultured H9c2 cells in 96-well plates and treated the cells differently. Then, we added 10 μL of CCK8 reagent (Dojindo Molecular Technologies, Kumamoto, Japan) to each well and mixed. The 96-well plate was placed in the incubator and incubated for another 2 h. We then used a microplate reader to detect the absorbance of each well at a wavelength of 450 nm and calculated cell viability with the absorbance.

Enzyme Linked Immunosorbent Assay (ELISA)

We detected the concentrations of inflammatory factors (LI-1β, IL-6, IL-8 and TNF-α) in rat serum and cell culture medium by ELISA kits (Thermo Fisher Scientific, Waltham, MA, USA). Firstly, we configure the standards and add them to the microplate. We then added the diluted sample to the microplate and added biotin antibody dilution to each well. After the mixture was incubated at 37°C for 60 min. We washed the microplate and added developer to each well for 20 min in the dark. Finally, we used a microplate reader to detect the absorbance of each well at a wavelength of 450 nm.

RNA Isolation and Quantitative Real-Time Reverse Transcription-Polymerase Chain Reaction (RT-PCR)

We used TRIzol reagent (Invitrogen, Carlsbad, CA, USA) to extract total RNA from rat myocardial tissue or H9c2 cells. We add 1 mL of TRIzol reagent to myocardial tissue or cells to fully lyse. We then added 200 μL of chloroform and collected the supernatant by centrifugation. We then added isopropanol and collected the precipitate. After washing the precipitate with absolute ethanol, we used RNase-free ddH_2O to dissolve the RNA. An ultraviolet spectrophotometer was used to detect the concentration of RNA. We used reverse transcription kits (Thermo Fisher Scientific, Waltham, MA, USA) to reverse RNA into cDNA. The reverse transcription system was 1 μg RNA + 2 μL Oligo (DT) 15 + 2 μL DNTP + RNase-free ddH_2O to 12 μL. CDNA was stored in a refrigerator at -20°C. Then, we used SYBR Green Mix (Vazyme, Nanjing, Jiangsu, China) for PCR. The PCR system was 12.5 μL SYBR Green Mix + 0.5 μL Forward Primer + 0.5 μL Reverse Primer + 0.5 μL ddH_2O + 2 μL cDNA. Endogenous U6 and GAPDH expression were used as controls. $2^{-\Delta\Delta Ct}$ was used to represent the relative expression of RNA. The primer sequences were shown in Table I.

Table I. RT-PCR sequence primers.

Name	Sense sequences (5'-3')	Anti-sense sequences (5'-3')
caspase3	GGAACGCGAAGAAAAGTG	ATTTTGAATCCACGGAGGT
FOXD3	CCCTCTCCACCCTCACC	GAAGCGCAACTCCTCACC
miR-486	ACACGAATTCTAACGGCTGTACTAG TGTGTGAGGG	ACACGAATTCTAACGGCTGTACTAGTGTG TGAGGG
U6	GCTTCGGCAGCACATATACTAAAAT	CGCTTCACGAATTTGCGTGTCAT
GAPDH	ATGGCTACAGCAACAGGGT	TTATGGGGTCTGGGATGG

Immunocytofluorescence (IF) Staining

We placed cell slides in 24-well plates and seeded H9c2 cells on the cell slides. After processing the cells, we took the 24-well plate and discarded the medium. Cells were then washed 3 times with phosphate-buffered saline (PBS). We then added 4% paraformaldehyde to each well for 15 min. After washing the cells with PBS, we added 0.01% TritonX-100 to each well for 15 min and washed the cells again. We then blocked the non-specific antigen with 10% goat serum for 1 h. After discarding goat serum, we incubated the cells at 4°C overnight using primary antibody dilution (FOXD3, ab64807, 1:500; caspase3, ab13847, 1:500, Abcam, Cambridge, MA, USA). We then washed the cells with PBS and incubated the cells for 1 h in the dark with fluorescent secondary antibody dilution (Abcam, Cambridge, MA, USA). Finally, we stained the nucleus with 4',6-diamidino-2-phenylindole (DAPI) and observed the staining results with a fluorescence microscope (LEICA, Koln, Germany).

Dual-Luciferase Reporter Assay

Targetscan system (http://www.targetscan.org/vert_72/) was used to predict the targets of miR-486. (Forkhead box D3) FOXD3 was found to be a potential target for miR-486. We used HEK 293T to verify the relationship between FOXD3 and miR-486. Firstly, we constructed a plasmid containing the luciferase reporter gene of the potential binding sequence of FOXD3 mRNA 3'-UTR and miR-486. We then transfected the plasmid into cells using Lipofectamine 3000. We then added 250 μl of Dual-Glo Luciferase Reagent (Thermo Fisher Scientific, Waltham, MA, USA) to the cells. After 10 min, we added Dual-Glo Stop & Glo Reagent to the cells. Finally, we used a microplate reader to measure the firefly luciferase fluorescence value.

Statistical Analysis

Statistical Product and Service Solutions (SPSS) 21.0 statistical software (IBM, Armonk, NY, USA) was used for statistical analysis. The data in this study were expressed as mean ±SD (standard deviation). Comparisons between groups were analyzed by analysis of variance, and pairwise comparisons within groups were analyzed by t-test. All experiments were repeated 3 times. $p<0.05$ indicated that the difference was statistically significant.

Results

Myocardium of IRI Rats Showed Low Expression of MiR-486

First, we made a rat model of IRI through coronary artery occlusion. HE staining (Figure 1A) revealed that the cardiomyocytes of the myocardial tissue in the infarcted area of IRI rats were disorderly arranged, and there was also a large number of inflammatory cell infiltrations between the cardiomyocytes. TTC staining (Figure 1B) showed the infarcted area of myocardial tissue, and the infarcted area of IRI rats was larger than that of normal rats. The concentration of myocardial injury markers (LDH and CK) represented the degree of myocardial injury. The concentrations of LDH (Figure 1C) and CK (Figure 1D) in the serum of IRI rats were significantly higher than those in normal rats. Then, we detected the concentrations of inflammatory factors (IL-1β, IL-6, IL-8 and TNF-α) in rat serum by ELISA (Figure 1E). The concentrations of inflammatory factors in the serum of IRI rats were significantly increased compared to normal rats. These results indicated that the IRI rat model was successfully made. Then, we detected the expression of miR-486 in rat myocardial tissue by RT-PCR (Figure 1F). The results showed that after myocardial IRI, miR-486 expression in rat myocardial tissue decreased.

MiR-486 Alleviated H/R-Induced H9c2 Cell Injury

We made an IRI model of H9c2 cells through H/R. RT-PCR detected (Figure 2A) the expression of miR-486 and FOXD3 in H9c2 cells. H9c2 cells in the H/R group expressed less miR-486

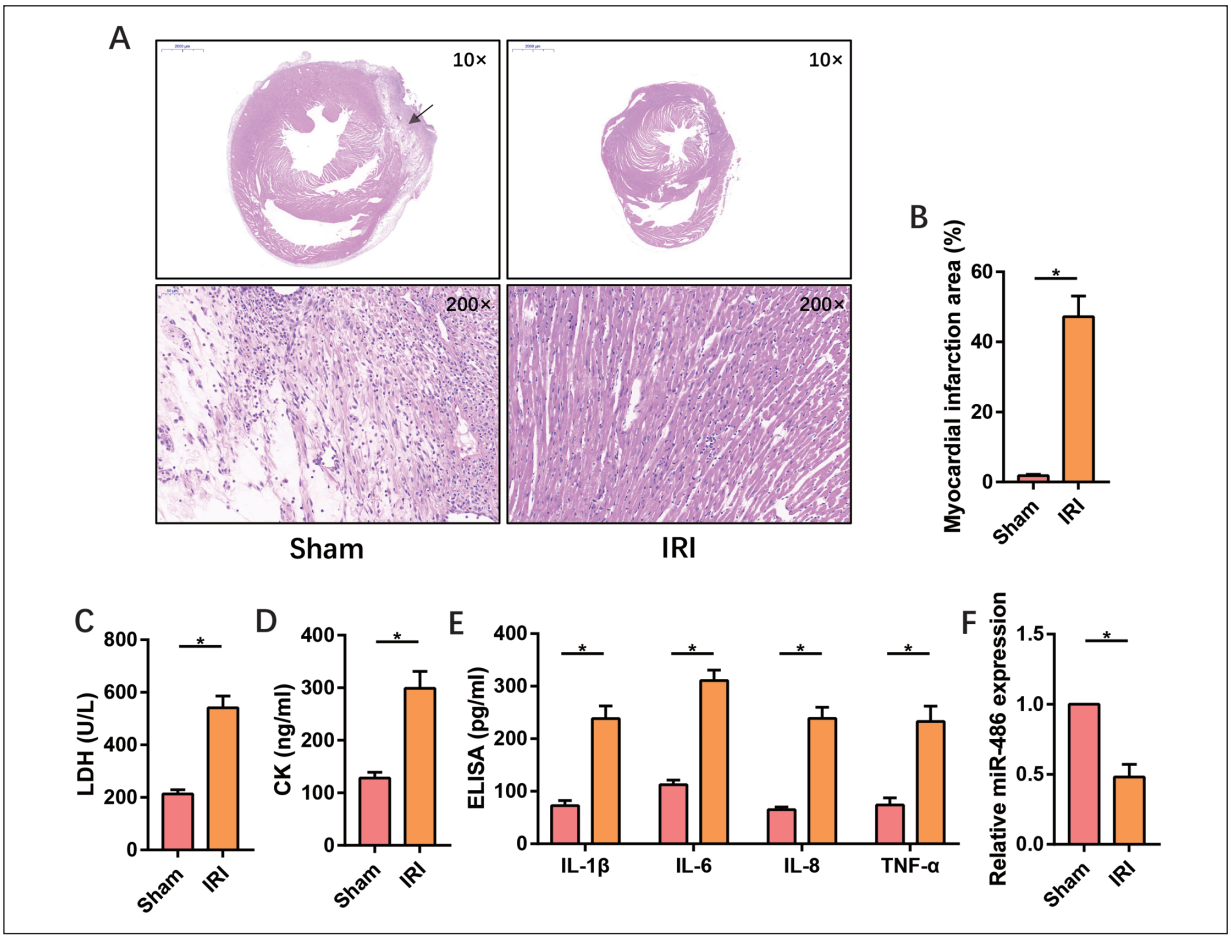

Figure 1. Myocardium of IRI rats showed low expression of miR-486. **A**, HE staining of myocardium in Sham group and IRI group (magnification: 10× and 200×). The arrow points to the area of injured myocardium; **B**, TTC staining of rat myocardium detected the myocardial infarction area; **C-D**, activity of LDH and CK in rat serum; **E**, IL-1β, IL-6, IL-8 and TNF-α in rat serum were detected by ELISA; **F**, miR-486 expression in rat myocardium was determined by RT-PCR. ("*" means the difference is statistically significant, $p<0.05$).

and more FOXD3. IF staining also detected the high expression of FOXD3 in the cells of the H/R group (Figure 2B). Then, we used agomir-control, agomir-miR-486, antagomir-control and antagomir-miR-486 to transfect H9c2 cells and detected the transfection efficiency by RT-PCR (Figure 2C). H9c2 cells are divided into 6 groups, including control group, H/R group, H/R + agomir-control group, H/R + agomir-miR-486 group, H/R + antagomir-control group and H/R + antagomir-miR-486 group. Firstly, we detected the viability of H9c2 cells by CCK8 assay (Figure 2D). Overexpression of miR-486 was found to increase the viability of H9c2 cells, whereas antagomir-miR-486 did the opposite. We then detected the concentration of inflammatory factors in the cell culture supernatant by ELISA (Figure 2E). The overexpression of miR-486 effectively reduced the concentrations of IL-1β, IL-6, IL-8 and TNF-α in the cell culture medium, while the inhibition of miR-486 exacerbated the level of cell inflammation. We detected the expression of the pro-apoptotic molecule caspase3 in H9c2 cells by IF staining (Figure 2F). The results showed that miR-486 can reduce the expression of caspase3.

FOXD3 is a Direct Target of MiR-486

To determine the mechanism of action of miR-486, we used Targetscan to predict the target of miR-486. FOXD3 was found to be a direct target of miR-486 (Figure 3A). We then used Dual-Luciferase reporter assay to verify the interaction of miR-486 and FOXD3. We transfected the Luciferase reporter vector of the sequence of FOXD3 3'-UTR of wild type (WT) or mutation (MUT) into HEK 293T cells (Figure 3B).

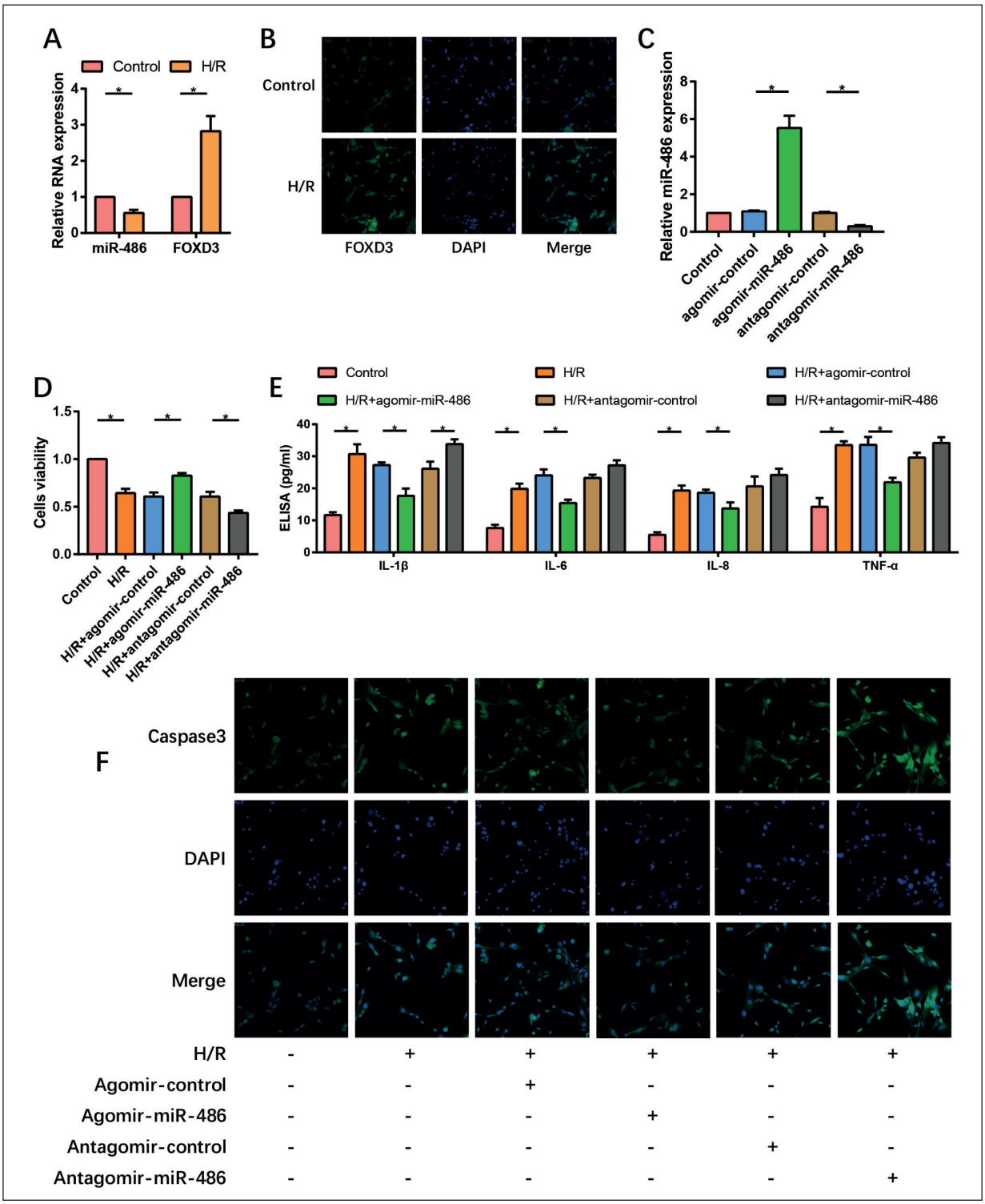

Figure 2. MiR-486 alleviated H/R-induced H9c2 cell injury. **A**, expression of miR-486 and FOXD3 in H9c2 cells was determined by RT-PCR; **B**, expression of FOXD3 protein was determined by IF staining (magnification: 200×); **C**, transfection efficiency was determined by RT-PCR; **D**, H9c2 cell viability was determined by CCK8 assay; **E**, IL-1β, IL-6, IL-8 and TNF-α in cell culture medium were detected by ELISA; **F**, expression of caspase3 protein was determined by IF staining (magnification: 200×). ("*" means the difference is statistically significant, $p<0.05$).

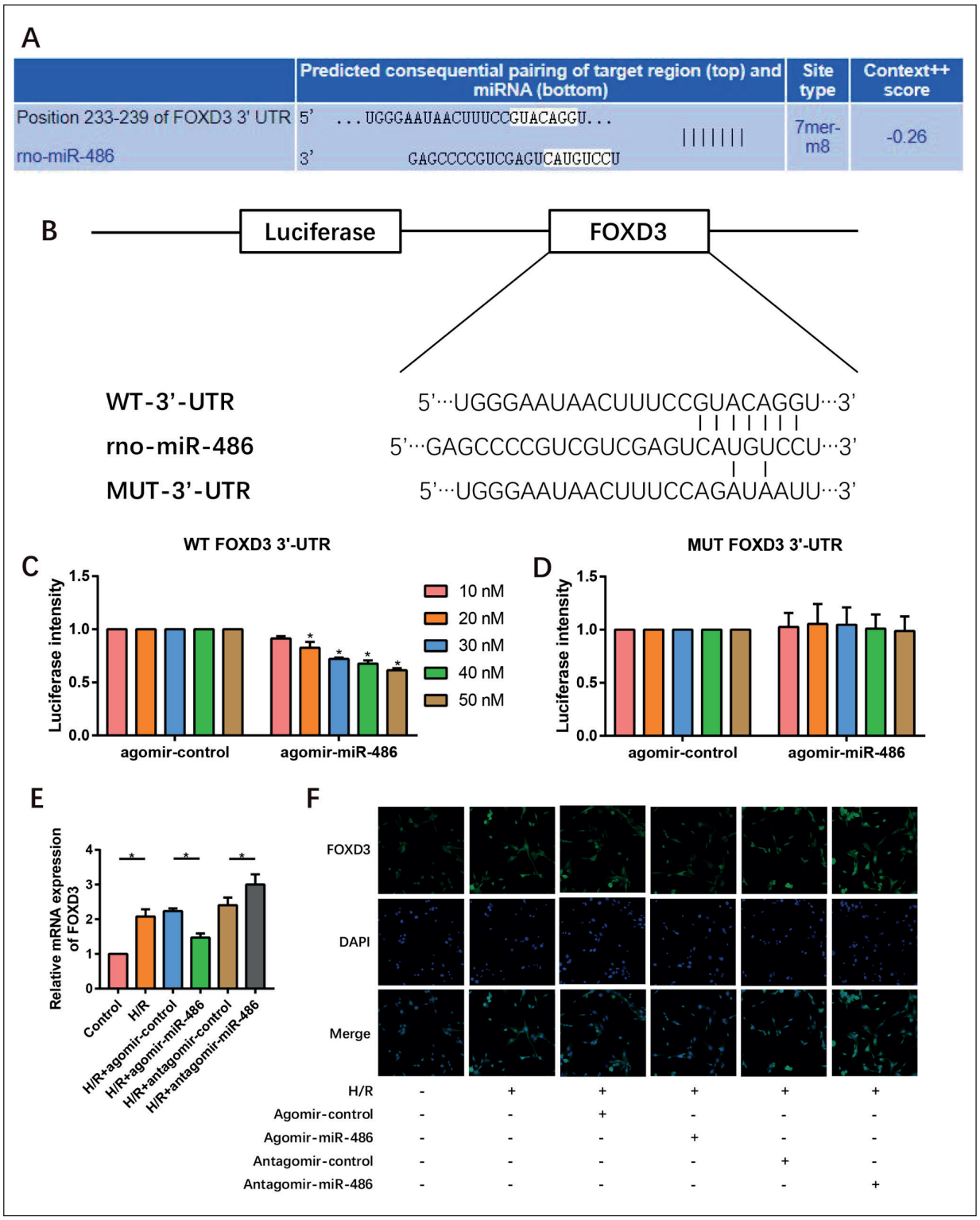

Figure 3. FOXD3 is a direct target of miR-486. **A**, targetscan predicted that FOXD3 is a potential target of miR-486; **B**, FOXD3 3'-UTR WT and MUT plasmid schematic; **C-D**, Dual-Luciferase reporter assay proved that miR-486 can bind and degrade FOXD3 mRNA; **E-F**, expression of FOXD3 mRNA and protein was determined by RT-PCR and IF staining (magnification: 200×). ("*" means the difference is statistically significant, $p<0.05$).

The results of the Dual-Luciferase reporter assay showed that the fluorescence intensity in HEK 293T cells co-transfected with WT-FOXD3 3'UTR and agomir-miR-486 was significantly decreased and concentration-dependent. However, the Luciferase activity of cells containing the mutated reporter gene was not significantly changed. This indicated that miR-486 directly targets the 3'-UTR of FOXD3 (Figure 3C, D). In addition, we detected the expression of FOXD3 mRNA (Figure 3E) and protein (Figure 3F) in H9c2 cells. After using agomir-miR-486 to promote miR-486 expression, the expression of FODX3 mRNA and protein decreased.

Overexpression of FOXD3 Reversed the Protective Effect of MiR-486 on H9c2 Cells

To determine the effect of FODX3 on H9c2 cells, we transfected FOXD3 overexpressing lentivirus in H9c2 cells. First, we checked the transfection efficiency by RT-PCR and Lenti-FOXD3 was found to increase the expression of FOXD3 in H9c2 cells (Figure 4A). Then, CCK8 assay found that the cell viability of H9c2 cells was reduced after FOXD3 was overexpressed. This indicated that overexpression of FOXD3 reversed the effect of miR-486 on the viability of H9c2 cells (Figure 4B). In addition, we detected the effect of FOXD3 on the level of inflammation in H9c2 cells by ELISA (Figure 4C). The results showed that FOXD3 attenuated the anti-inflammatory effects of miR-486. IF staining detected caspase3 expression and FOXD3 was found to promote caspase3 expression (Figure 4D).

Discussion

IRI is a pathophysiological process that mainly occurs during the transition from the ischemic phase to the reperfusion phase. The mechanism

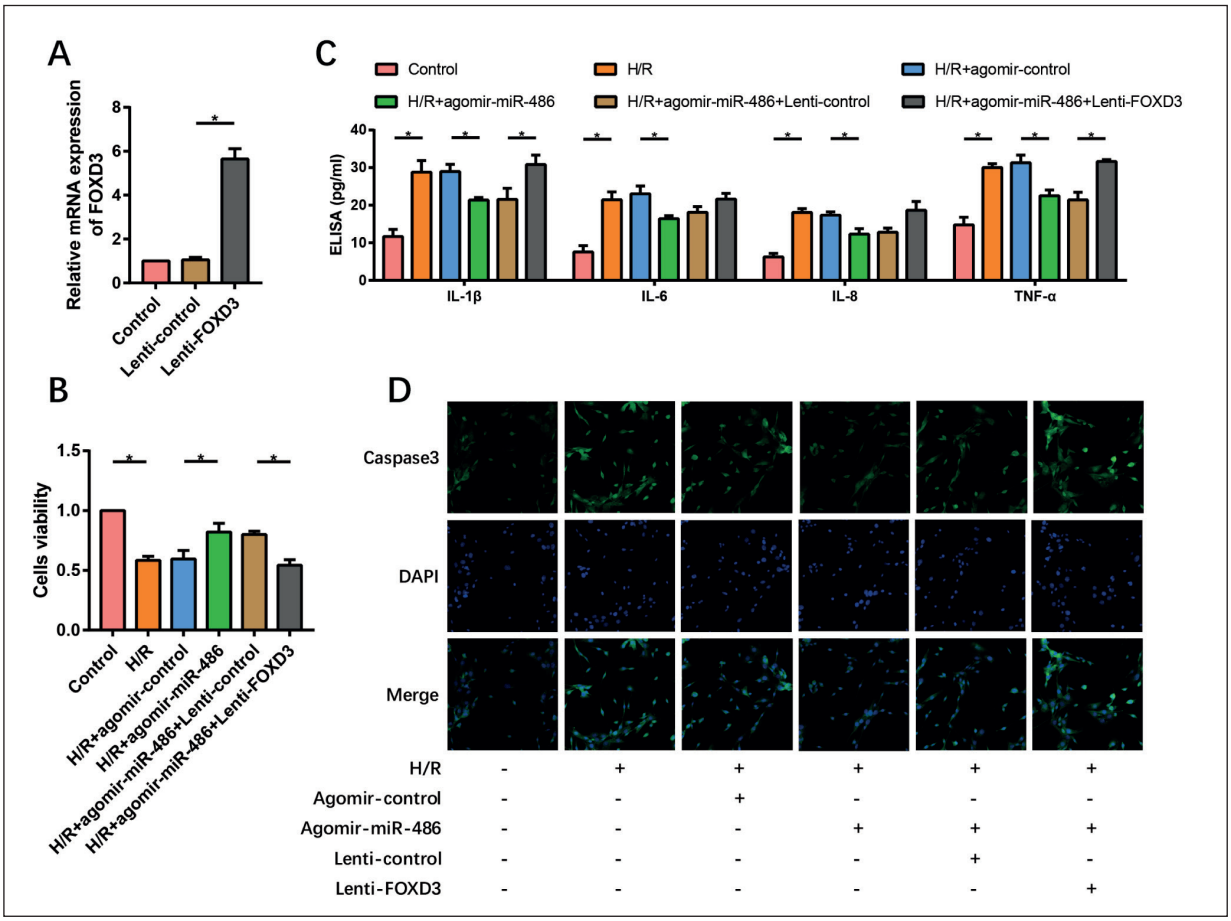

Figure 4. Overexpression of FOXD3 reversed the protective effect of miR-486 on H9c2 cells. **A**, transfection efficiency of lentivirus was determined by RT-PCR; **B**, H9c2 cell viability was determined by CCK8 assay; **C**, IL-1β, IL-6, IL-8 and TNF-α in cell culture medium were detected by ELISA; **D**, expression of caspase3 protein was determined by IF staining (magnification: 200×). ("*" means the difference is statistically significant, $p<0.05$).

by which IRI occurs is not fully understood[13]. The current evidence-based mechanisms include oxidative stress, intracellular calcium overload, vascular endothelial damage, endoplasmic reticulum stress, and inflammatory responses[14]. We successfully made an IRI rat model through coronary artery occlusion and found that the expression of miR-486 in myocardial tissue of IRI rats was lower than that of the control group. This shows that miR-486 has an important role in myocardial IRI. Overexpression of miR-486 not only increased the viability of H9c2 cells, but also reduced the levels of inflammation and apoptosis of the cells. Therefore miR-486 plays an important role in the resistance of cardiomyocytes to IRI. We found that FOXD3 is a direct target of miR-486, and overexpression of FOXD3 attenuated the protective effect of miR-486 on H9c2 cells. Therefore, miR-486 may play a role in protecting myocardial cells from IRI by regulating FOXD3.

With the deepening of research on myocardial IRI, more and more evidence showed that the inflammatory response is activated during the myocardial ischemic phase, and reperfusion further exacerbates the inflammatory response in the myocardium[15]. Neutrophil-based inflammation is one of the important mechanisms causing myocardial IRI. In addition, some clinical studies have also found that after revascularization of myocardial infarction, inflammatory factors in patients' serum, including TNF-α, IL-1β, IL-6, and IL-8, have significantly increased. In the absence of oxygen and nutritional supply, damage to a large amount of myocardial tissue leads to inflammatory response, which initiates the heart repair process[16]. Given IRI occurs without microorganisms, this inflammatory response is aseptic inflammation. However, the post-IRI inflammatory response is similar to that of pathogen invasion. Both of them include chemotaxis, infiltration of inflammatory cells, and secretion of inflammatory factors. Although various cell types mediate the inflammatory response after IRI, white blood cells in the blood play a particularly prominent role[17]. Neutrophils and coronary endothelial cells exhibit specific interactions during early reperfusion. In the early minutes of reperfusion, neutrophils were recruited into reperfusion myocardial tissue by the release of pro-inflammatory factors (TNF-α, IL-6, platelet activating factor, alexin and leukotriene B4) and chemokines (IL-8)[18]. Endothelial cells are then activated, and cell adhesion molecules are rapidly upregulated, such as P-selectin and E-selectin. Cell adhesion molecules promote leukocyte adhesion and allow them to infiltrate into damaged tissue. Infiltrated neutrophils engulf cell debris, release proteolytic enzymes and produce reactive oxygen species to degrade the extracellular matrix[19]. In addition, the release of inflammatory factors from neutrophils results in the reduction of endothelium-derived relaxing factors, NO and prostacyclin. This promotes coronary microthrombosis and disrupts the integrity of the microvascular bed, leading to increased coronary resistance and impaired microcirculatory function[20]. Therefore, further elucidating the specific mechanism of inflammation in IRI and exploring potential therapeutic targets are the keys to improving the prognosis of myocardial IRI and improving the clinical efficacy of patients with ischemic heart disease. Our study found that miR-486 can reduce the expression of inflammatory cytokines and chemotaxis-related cytokines in rat cardiomyocytes induced by IRI, suggesting that miR-486 may reduce IRI-induced myocardial injury through anti-inflammatory effects.

FOXD3 belongs to the forkhead protein family. FOXD3 plays an important role in maintaining pluripotent differentiation of mammalian neural crests[21]. FOXD3 is not only expressed in mouse embryonic stem cells and embryoma, but also in mouse epidermis and neural crest cells at later stages of embryonic development[22]. In FOXD3 knockout embryos, trophoblast precursor cells cannot self-renew, however, the number of embryonic trophoblastic cells increased excessively[22]. Zhang et al[23] have shown that FOXD3 can bind to the IL-10 promoter and limit the activation of the IL-10 promoter, thereby inhibiting the anti-inflammatory effect of IL-10. However, there are no reports on the role of FOXD3 in cardiomyocytes. Our study found that FOXD3 is a direct target of miR-486. MiR-486 plays a role in regulating cardiomyocytes by degrading FOXD3. We found that the overexpression of FOXD3 reduced the protective effect of miR-486 on cardiomyocytes by transfecting FOXD3 overexpression lentivirus in H9c2 cells. Therefore, the increase of FOXD3 caused by the decrease of miR-486 in myocardial tissue of IRI rats may be one of the factors that cause IRI. Therefore, miR-486 may become a therapeutic target for myocardial IRI in the future. We hope that our study can provide a strong theoretical basis for the treatment of myocardial IRI.

Conclusions

The expression of miR-486 was low in rat myocardial tissue after IRI. MiR-486 binds and degrades FOXD3 mRNA, thereby reducing the level of inflammation and apoptosis in cardiomyocytes. Therefore, miR-486 may be used as a therapeutic target for IRI and used to alleviate myocardial IRI.

Conflict of Interests

The authors declare that they have no conflict of interest.

References

1) Kapur NK, Reyelt L, Swain L, Esposito M, Qiao X, Annamalai S, Meyns B, Smalling R. Mechanical Left Ventricular Unloading to Reduce Infarct Size During Acute Myocardial Infarction: Insight from Preclinical and Clinical Studies. J Cardiovasc Transl Res 2019; 12: 87-94.
2) Safi S, Sethi NJ, Nielsen EE, Feinberg J, Jakobsen JC, Gluud C. Beta-blockers for suspected or diagnosed acute myocardial infarction. Cochrane Database Syst Rev 2019; 12: D12484.
3) Kaier TE, Alaour B, Marber M. Cardiac Myosin-Binding Protein C-From Bench to Improved Diagnosis of Acute Myocardial Infarction. Cardiovasc Drugs Ther 2019; 33: 221-230.
4) Reed GW, Rossi JE, Cannon CP. Acute myocardial infarction. Lancet 2017; 389: 197-210.
5) Castro-Dominguez Y, Dharmarajan K, McNamara RL. Predicting death after acute myocardial infarction. Trends Cardiovasc Med 2018; 28: 102-109.
6) Herr DJ, Singh T, Dhammu T, Menick DR. Regulation of metabolism by mitochondrial enzyme acetylation in cardiac ischemia-reperfusion injury. Biochim Biophys Acta Mol Basis Dis 2020; 1866: 165728.
7) Bencsik P, Gomori K, Szabados T, Santha P, Helyes Z, Jancso G, Ferdinandy P, Gorbe A. Myocardial ischaemia reperfusion injury and cardioprotection in the presence of sensory neuropathy: Therapeutic options. Br J Pharmacol 2020; 177: 5336-5356.
8) Waheed S, Zeng L. The Critical Role of miRNAs in Regulation of Flowering Time and Flower Development. Genes (Basel) 2020; 11: 319.
9) ElKhouly AM, Youness RA, Gad MZ. MicroRNA-486-5p and microRNA-486-3p: Multifaceted pleiotropic mediators in oncological and non-oncological conditions. Noncoding RNA Res 2020; 5: 11-21.
10) Chai X, Si H, Song J, Chong Y, Wang J, Zhao G. miR-486-5p Inhibits Inflammatory Response, Matrix Degradation and Apoptosis of Nucleus Pulposus Cells through Directly Targeting FOXO1 in Intervertebral Disc Degeneration. Cell Physiol Biochem 2019; 52: 109-118.
11) Lopez-Bertoni H, Kotchetkov IS, Mihelson N, Lal B, Rui Y, Ames H, Lugo-Fagundo M, Guerrero-Cazares H, Quinones-Hinojosa A, Green JJ, Laterra J. A Sox2:miR-486-5p Axis Regulates Survival of GBM Cells by Inhibiting Tumor Suppressor Networks. Cancer Res 2020; 80: 1644-1655.
12) Chou ST, Peng HY, Mo KC, Hsu YM, Wu GH, Hsiao JR, Lin SF, Wang HD, Shiah SG. MicroRNA-486-3p functions as a tumor suppressor in oral cancer by targeting DDR1. J Exp Clin Cancer Res 2019; 38: 281.
13) Shi B, Ma M, Zheng Y, Pan Y, Lin X. mTOR and Beclin1: Two key autophagy-related molecules and their roles in myocardial ischemia/reperfusion injury. J Cell Physiol 2019; 234: 12562-12568.
14) Cadenas S. ROS and redox signaling in myocardial ischemia-reperfusion injury and cardioprotection. Free Radic Biol Med 2018; 117: 76-89.
15) Pei YH, Chen J, Wu X, He Y, Qin W, He SY, Chang N, Jiang H, Zhou J, Yu P, Shi HB, Chen XH. LncRNA PEAMIR inhibits apoptosis and inflammatory response in PM2.5 exposure aggravated myocardial ischemia/reperfusion injury as a competing endogenous RNA of miR-29b-3p. Nanotoxicology 2020; 14: 638-653.
16) Carbone F, Bonaventura A, Montecucco F. Neutrophil-Related Oxidants Drive Heart and Brain Remodeling After Ischemia/Reperfusion Injury. Front Physiol 2019; 10: 1587.
17) Jensen RV, Andreadou I, Hausenloy DJ, Botker HE. The Role of O-GlcNAcylation for Protection against Ischemia-Reperfusion Injury. Int J Mol Sci 2019; 20: 404.
18) Toldo S, Mauro AG, Cutter Z, Abbate A. Inflammasome, pyroptosis, and cytokines in myocardial ischemia-reperfusion injury. Am J Physiol Heart Circ Physiol 2018; 315: H1553-H1568.
19) Ong SB, Hernandez-Resendiz S, Crespo-Avilan GE, Mukhametshina RT, Kwek XY, Cabrera-Fuentes HA, Hausenloy DJ. Inflammation following acute myocardial infarction: Multiple players, dynamic roles, and novel therapeutic opportunities. Pharmacol Ther 2018; 186: 73-87.
20) Toldo S, Abbate A. The NLRP3 inflammasome in acute myocardial infarction. Nat Rev Cardiol 2018; 15: 203-214.
21) Rosenbaum SR, Knecht M, Mollaee M, Zhong Z, Erkes DA, McCue PA, Chervoneva I, Berger AC, Lo JA, Fisher DE, Gershenwald JE, Davies MA, Purwin TJ, Aplin AE. FOXD3 Regulates VISTA Expression in Melanoma. Cell Rep 2020; 30: 510-524.
22) Xiao L, Shan Y, Ma L, Dunk C, Yu Y, Wei Y. Tuning FOXD3 expression dose-dependently balances human embryonic stem cells between pluripotency and meso-endoderm fates. Biochim Biophys Acta Mol Cell Res 2019; 1866: 118531.
23) Zhang Y, Wang Z, Xiao H, Liu X, Zhu G, Yu D, Han G, Chen G, Hou C, Ma N, Shen B, Li Y, Wang T, Wang R. Foxd3 suppresses interleukin-10 expression in B cells. Immunology 2017; 150: 478-488.